

Power Matching Approach for GPS Coverage Extension

Samer S. Saab, *Senior Member, IEEE*, and Zaher M. Kassas, *Student Member, IEEE*

Abstract—The inherent problem of the Global Positioning System (GPS), which is signal obstruction, remains the major obstacle that inhibits it from functioning as a “reliable stand-alone” positioning system. Therefore, it is becoming a common practice to couple the GPS system with an external positioning system whenever the GPS receiver is expected to operate in regions of dense canopy, such as urban areas. Commercial automobile navigation systems currently employ a GPS receiver coupled with a dead reckoning (DR) system and a map-matching algorithm. Most DR systems, which compensate for GPS inaccuracies and frequent GPS signal obstructions, employ an odometer and a directional sensor. In this paper, a power matching approach is proposed for GPS coverage extension in urban area. The algorithm, based on a statistical measure, correlates the received power from different GPS satellite vehicles (SVs), which leads to a specific signature, i.e., to a topographical database with periodic time-varying estimates of the received powers of SVs. An experimental approach is presented to examine the feasibility of applying the proposed positioning system.

Index Terms—Global Positioning System, power matching, terrain mapping.

I. INTRODUCTION

POSITIONING systems can be divided into two categories, namely 1) self-positioning systems and 2) remote positioning systems. As their names suggest, in self-positioning systems [e.g., Global Positioning System (GPS)], the objects themselves determine where they are. In remote positioning systems (e.g., radar), a central operations center determines the location of the vehicles [1]. Self-positioning systems can be divided into three location technologies [2], namely 1) stand alone [e.g., dead reckoning (DR)], 2) satellite based (e.g., GPS), and 3) terrestrial radio based (e.g., LORAN-C). A framework for positioning, navigation, and tracking problems is presented in [3], [4]. Another class of positioning systems is a hybrid system employing two or more of these technologies with possible addition of specific sensors and a map-matching system. Map matchers correlate specific observed position details estimated by the on-board sensors to stored details directly related to different known locations. An on-board computer calculates the autocorrelation function between specific measured position characteristics and the potential stored characteristics. The

course associated with the highest autocorrelation would then be considered as a candidate for the actual location.

Map matching is applied to a wide variety of vehicular navigation. Marine vehicles determine the contour of the seafloor with sonar and compare the measured profile to stored maps. Aircraft and cruise missiles measure the vertical profile of the terrain below the vehicle with respect to a certain reference and match it to a stored profile. For train-like applications, a novel map-matching approach was proposed, which takes full advantage of the inherited one-dimensional (1-D) train track [5], [6]. For mobile robots and other land vehicle navigation, TV cameras have been employed to observe edges of recognizable objects [7], [8].

The most common application of map matching is employed for automobile navigation. The basic system design uses a measurement of the distance traveled along with heading changes from DR systems [9]–[11], and other systems combine the GPS with DR systems [12]–[19]. These systems typically use a fusion of sensors, in particular, GPS receiver, odometer, directional sensor (e.g., gyro), digital map database, and different signal processing algorithms [20]–[23].

Even if differential GPS (DGPS) is employed, DR and map matching should be implemented to compensate for DGPS “failures” (and GPS inaccuracies if GPS without differentiation is assumed). In this context, GPS failure means the inability of a GPS receiver to estimate its position. In general, GPS failures occur whenever the signals transmitted by most of the GPS satellite vehicles (SVs) are obstructed or when the dilution of precision (DOP) factors are large. Recent research directions in the weak signal processing area aims to allow the GPS receiver to estimate its position with lower signal-to-noise ratios (SNRs), hence, extending the GPS coverage area [24]–[27].

Based on the design of the GPS satellite layout, failures do not take place in ideal open space vicinity. Thus, the surroundings of a GPS receiver play an important role. In particular, if the vicinity of the GPS receiver does not obstruct the GPS SV signals, then a DR system will not be needed. However, at a fixed time, the GPS receiver antenna vicinity may obstruct one or more SV signals. Such obstructions depend on two variables, namely 1) the layout of the neighborhood and 2) the time. Because the orbit of the GPS SVs is periodic, one can easily predict the locations of all SVs at all times. In addition, if a three-dimensional (3-D) map of a sufficiently “small” area is available, then one can estimate the received powers of all accessible SVs at a certain point, which leads to a unique signature of the received power of all the different SVs [28]. Consequently, if the received powers of all accessible SVs are available, then the location of the receiver within a sufficiently

Manuscript received February 23, 2004; revised January 6, 2005 and September 13, 2005. The Associate Editor for this paper was S. Tang.

S. S. Saab is with the Department of Electrical and Computer Engineering, Lebanese American University, Byblos 48328, Lebanon (e-mail: ssaab@lau.edu.lb).

Z. M. Kassas is with National Instruments, Austin, TX 78759 USA (e-mail: zkassas@ieee.org).

Digital Object Identifier 10.1109/TITS.2006.874720

small area can be recovered. This is the concept investigated in this paper. To assess the practicality of this notion from a theoretical approach, many variables need to be addressed, which may lead to a rather complex analysis. Therefore, in this paper, an experimental approach is selected to examine the feasibility of applying this novel idea. In addition, a power-matching algorithm, which is based on statistical measure, is presented. It is worth noting that this approach can also take advantage of weak GPS signal processing to further extend the GPS coverage area.

The paper is organized as follows: Section II presents the necessary background for the proposed method. Section III describes the proposed methodology and presents the power-matching algorithm. In Section IV, experimental results are presented and analyzed. Concluding remarks and future work are summarized in Section V.

II. BACKGROUND

A. GPS Signals

The accuracy of the GPS position, velocity, and time (PVT) solution depends on a complicated interaction of various factors. In general, the accuracy of the PVT solution depends on the quality of the SV ephemeris data as well as on the pseudo-range measurements [29]–[32].

In this paper, three regions will be defined. The clear region (CR) is the region in which the DOP is significant for position estimation. The partially dark (PD) region is the region in which the SNR of at least one received GPS signal is notable. The totally dark (TD) region is the region in which all received SV signals are “negligible.” Actually, the PD region is very common in urban areas, where tall buildings may easily obstruct the line-of-sight (LOS) between the GPS SV and the GPS receiver antenna. On the other hand, the TD region is common whenever the GPS receiver roves inside a building or a tunnel.

The power intercepted by the GPS receiver antenna will be categorized into two levels, namely 1) the power intercepted from LOS signals and 2) the power intercepted from non-LOS signals. The LOS signal interception occurs due to the “direct” propagation of the signal from the GPS SV to the GPS receiver, whereas the non-LOS signal interception occurs due to the diffraction or reflection of the GPS signal from nearby objects. Usually, the power intercepted by the GPS receiver antenna from the LOS signals is more significant than that intercepted from the non-LOS signals.

B. GPS SV Orbits

The orbital period of the GPS SV around the earth is 11 h and 58 min [29], whereas the orbital period of the earth around itself is about 24 h. Hence, it can be concluded that a given SV sky-plot will show again every 23 h and 56 min. In other words, if we have a sky-plot consisting of a total of six GPS SVs, for example, above us now, then we can expect the same sky-plot with the same six SVs at the same locations above us after Δt , with Δt being 23 h and 56 min. For further information on the characteristics of the GPS SV signals, the reader is referred to [28], [33], and [34].

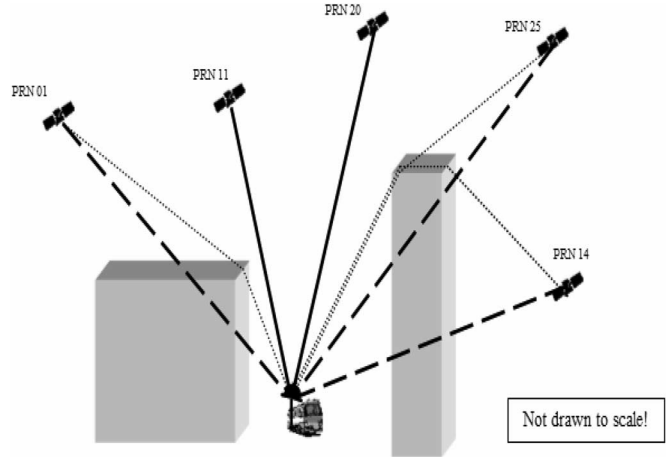


Fig. 1. Buildings obstructing the LOSs between GPS SVs and a GPS receiver.

III. PROPOSED POWER-MATCHING ALGORITHM

A. Motivation

The incentives leading to the hypothesis that the GPS system could cover PD regions are established in this subsection. One of the key concepts motivating this hypothesis is the fact that the orbital period of the GPS SV is 11 h and 58 min. Consequently, the constellation of the GPS SVs will maintain their previous locations (elevations and azimuths) after Δt . The power of the signal received by the GPS receiver from each GPS SV depends on the background noise at the GPS receiver proximity as well as on the presence of nearby objects obstructing the LOSs between the GPS SVs and the GPS receiver. Accordingly, if a nearby object is present within the LOS between the GPS SV and the GPS receiver, the signal power received from that SV would drop significantly, thus lowering the SNR value. If the power received falls below a certain threshold, the SNR value will be reported by the NMEA output message as a null string (value of zero).

A common problem of a GPS navigator is considered. Suppose that a GPS receiver is roving in a PD region. However, the GPS receiver cannot produce a PVT solution because it cannot use a sufficient number of SVs due to low SNR values. Recalling that the same constellation of GPS SVs maintains (approximately) their current positions after Δt and that the power values depend on the proximity environment of the GPS receiver, it should be expected that if the GPS receiver returns to the same PD region after Δt , it should encounter comparable power values. In particular, the GPS receiver should report relatively the same power values for the available GPS SVs in both days, provided that the GPS receiver would follow the “same” track in both days with a time offset Δt .

To further illustrate this notion, a specific pattern depicted in Fig. 1 is considered. In this particular situation, there are five GPS SVs, denoted as PRN 01, PRN 11, PRN 14, PRN 20, and PRN 25. Furthermore, there is a GPS receiver mounted on a bus and roving between two buildings. It could be seen in the figure that there is a clear LOS between the GPS receiver and two of the GPS SVs, namely 1) PRN 11 and 2) PRN 20. However, the two buildings obstruct the LOSs between the GPS receiver and the three other GPS SVs, namely 1) PRN 01, 2) PRN 14, and

3) PRN 25. The power values of PRN 11 and PRN 20 are much larger than the ones associated with PRN 01 and PRN 25, and the power values of PRN 01 and PRN 25 are much larger than the one of PRN 14. Nevertheless, if the bus was on the right or left of the two buildings, then the order of magnitude of these power values would be completely different. This fact yields different power signatures corresponding to different locations. Should the bus return to the same location after Δt , the five GPS SVs should maintain their “current” locations, and the receiver should report relatively the same power values for the five available SVs. With the aid of this information, the GPS receiver would be capable of identifying its location as it enters this PD region based solely on the GPS system and without needing to refer to any external sensors.

A singularity arises if the GPS receiver would report the same power values for all SVs in “nearby” PD regions. This would cause confusion about the true position in which the GPS receiver is roving. On the contrary, it would cause no confusion if the power values for all available SVs at a certain time happen to be “relatively” identical in more than one far-apart PD regions, as power-matching techniques could resolve this dilemma. Power matching is based on a premise that the vehicle could be nowhere but on a road. The vehicle most recent route history together with the latest estimates of position and velocity from the positioning system could be used by the power-matching algorithm to find the likeliest road segment from its stored database and places the vehicle on the “correct” road segment. It is unlikely that the GPS receiver would loose lock for a very long time. Therefore, as soon as the GPS receiver would loose lock, it would use its most recent route history together with the latest PVT solution to zoom on the region in which it is roving [1].

Because the power values depend directly on the proximity environment in which the GPS receiver is roving, it should be expected that the power values reported by the GPS receiver to be compatible if it happens that there exist identical regions in terms of geometry, provided that the power level of the background noise in those regions is close. Fortunately, this is not the case in urban areas due to the irregular and asymmetrical building distribution. Even in the case of parallel streets, where identical geometry might exist within the same proximity, the GPS receiver cannot move from one street to another by jumping around, and it is forced to turn. Fortunately, turning left or right would change the geometry of the surrounding environment, thus changing the power values, and hence, enabling the GPS receiver to identify its position. Another class of singularities is when the GPS receiver is roving within a TD region (e.g., inside a tunnel). In this case, the system would only report the position to be somewhere inside this specific TD region. If the speed estimate of the GPS receiver is available before entering this TD region, then this speed can be assumed constant and integrated to give an estimate of the distance traveled within this region. Unfortunately, the model for the associated error would possess random walk characteristics. It is worth noting that in the case where one of the SVs is not operational, the corresponding SNR would be zero. Consequently, the proposed system would disregard this particular SV.

B. Development of the Proposed Algorithm

In this subsection, a power-matching algorithm is proposed, where the measurements of the signal power from different SVs are matched to their corresponding estimated values. The nominal values are assumed to be estimated based on a 3-D map or a topographic database of the GPS receiver neighborhood at the time when the measurements are acquired. Similar to the one employed in Durkin’s model, the topographical database of an urban area can be thought of as a 2-D array. Each array element corresponds to a point on a service area map. The contents of each element include the elevation and type of object. As presented in Section II, at each instant, the position of all SVs can be obtained. By making use of the topographic database and field strength prediction model the power of the available SVs at different relative positions of the receiver neighborhood can be estimated. A typical statistical model for this class of application, where the LOS path is blocked, is the urban three-state fade model (UTSFM) developed in [35]. The parameters of this model are also estimated from measurement made outdoors with GPS receivers in the urban Calgary and Vancouver, Canada [36]. Given a specific location in a PD region at time t , GPS SV position, and information about the surrounding objects (from the topographic database) in the PD region, by using one of the classical propagation prediction models, the “nominal” signal power of existing SVs can be estimated. The outcome of this model, that is, the estimated signal power at time t corresponding to each available SV, is stored in a row of an information matrix $M(t)$, along with the respective position (in the vicinity of the receiver) and the available GPS SV PRNs (see Fig. 2).

The proposed algorithm correlates the measured signal power with its corresponding estimated one based on a statistical model. The location corresponding to the highest correlation is considered to be a candidate to the position under investigation.

Notations: Let $S_{ij}(t)$ denote the nominal value of the received signal power of the j th SV, $1 \leq j \leq n$, at location i , $1 \leq i \leq m$, and let $\hat{S}_j(t)$ denote the measured signal power obtained by the GPS receiver of the j th SV, where n is the number of SVs, and m is the number of the surveyed locations in the vicinity of the GPS receiver under examination. Define the mean absolute error as follows:

$$\Delta S_i(t) \equiv \frac{1}{n} \sum_{j=1}^n \left| S_{ij}(t) - \hat{S}_j(t) \right|.$$

Fig. 3 illustrates the proposed power-matching algorithm, where the time argument t is dropped for compactness of presentation. The proposed algorithm correlates the average of the measured signal power to their corresponding surveyed values by first computing ΔS_i , $1 \leq i \leq m$, and then choosing the location corresponding to k such that $\Delta S_k = \min_i [\Delta S_i]$, $1 \leq i \leq m$. Subsequently, a reliability test is performed. Based on a probabilistic measure indicating the probability of prediction error, a tolerance value δs is chosen. If $\Delta S_k \leq \delta s$, the estimate corresponding to the k th position is selected, otherwise, the position prediction is rejected.

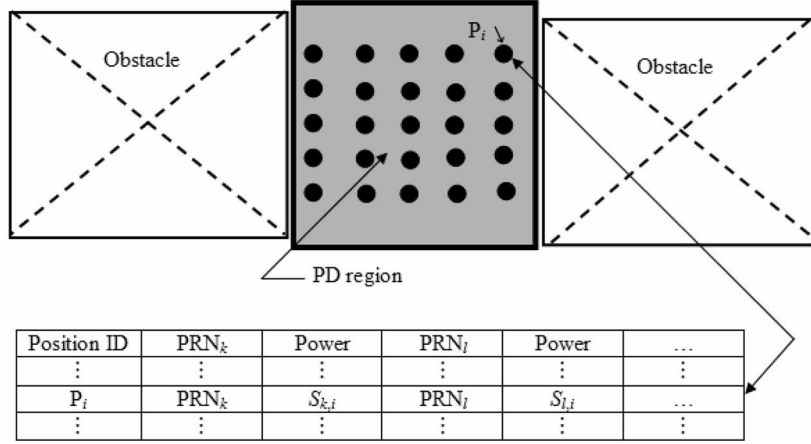


Fig. 2. Illustration of a surveyed PD region at time t and the corresponding information matrix $M(t)$.

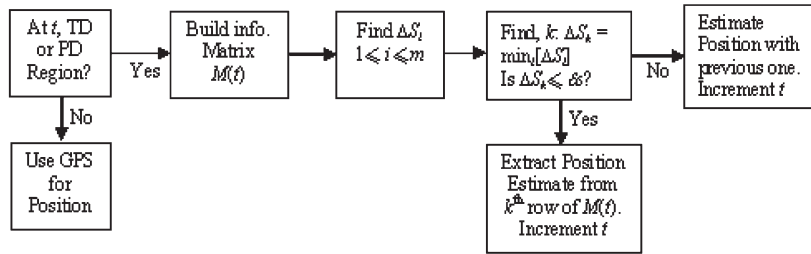


Fig. 3. Proposed power-matching algorithm.

Derivation of the Probability Density Function $\Delta S_i(t)$: Assume that the power value for a specific GPS receiver is normalized such that the maximum power is equal to A and the minimum power is equal to 0. That is, $0 \leq S_{ij}(\cdot) \leq A$, for all i and j . There are several significant *independent* sources of errors that are associated with $\hat{S}_j(t)$.

- 1) Quantizing errors e_{Q_j} : Most likely, the location of the receiver under investigation is different than the location of all the finite number of “surveyed” locations, which are used in building the information matrix $M(t)$, in the PD region. This will result in a quantizing error. Let d be the maximum distance between any two adjacent surveyed locations. The statistical distribution of such class of errors, for sufficiently small d , can be approximated as white and uniformly distributed in $[-A/q, A/q]$, where the constant $q > 1$ is a normally decreasing function of the spacing between the surveyed locations. It follows that the standard deviation of e_{Q_j} is $\sigma_Q = (A^2/3q^2)^{1/2}$.
- 2) Modeling errors e_{M_j} : These errors are due to modeling errors while estimating the received signal power of the surveyed locations in matrix $M(t)$. This class of modeling errors is assumed to be white and normally distributed with zero-mean and standard deviation σ_M .
- 3) Thermal noise e_{T_j} : This is due to the corresponding electronic components that contribute to the noise level seen at the detector output of the receiver. Typically, this is modeled as a zero-mean white Gaussian noise with standard deviation σ_T .

Consequently, $S_{ij}(t) - \hat{S}_j(t) = e_{Q_j}(t) + e_{M_j}(t) + e_{T_j}(t)$. Next, the statistical properties of $\Delta S_i(\cdot)$ are studied for every fixed

time instant t . The time argument t is dropped for compactness of presentation. Thus

$$\Delta S_i = \frac{1}{n} \sum_{j=1}^n |e_{Q_j} + e_{M_j} + e_{T_j}|.$$

For $1 \leq j \leq n$, $|e_{Q_j} + e_{M_j} + e_{T_j}|$ are identically distributed. Therefore, for $n > 2$, ΔS_i can be approximated to have normal distribution. To describe its probability distribution (pdf), the mean $m_{\Delta S}$ and standard deviation $\sigma_{\Delta S}$ must be computed as a function of n , σ_Q , σ_M , and σ_T .

Because e_M and e_T are considered zero-mean normally distributed and independent random variables, $(e_{M_j} + e_{T_j})$ is also zero-mean normally distributed with standard deviation $= (\sigma_M^2 + \sigma_T^2)^{1/2}$. Next, the pdf of $(e_{M_j} + e_{T_j} + e_{Q_j})$ is examined. Again, because $(e_{M_j} + e_{T_j})$ and e_{Q_j} are zero-mean and independent, $(e_{M_j} + e_{T_j} + e_{Q_j})$ is also zero-mean with standard deviation $(\sigma_M^2 + \sigma_T^2 + \sigma_Q^2)^{1/2}$. It is well known that the pdf of two independent random variables is the convolution of their associated pdfs. For this case, the pdf of $(e_{M_j} + e_{T_j} + e_{Q_j})$ is the convolution of the “bell” curve with variance $= \sigma_M^2 + \sigma_T^2$ and a pulse function with a width of $2\sqrt{3}\sigma_Q$ and an amplitude of $(2\sqrt{3}\sigma_Q)^{-1}$. Thus

$$f_Z(z) = \frac{1}{2\sqrt{6}\pi\sigma_1} \int_{\frac{z-\sqrt{3}\sigma_1/2}{\sigma_2}}^{\frac{z+\sqrt{3}\sigma_1/2}{\sigma_2}} e^{-t^2/2} dt$$

where $z = e_{M_j} + e_{T_j} + e_{Q_j}$, $\sigma_1 = \sigma_Q$, and $\sigma_2 = (\sigma_M^2 + \sigma_T^2)^{1/2}$. It turns out that whenever $(\sigma_M^2 + \sigma_T^2)^{1/2}$ is notably greater than σ_Q , the pdf of $(e_{M_j} + e_{T_j} + e_{Q_j})$ can be approximated with a zero-mean normally distributed random variable with standard deviation $(\sigma_M^2 + \sigma_T^2 + \sigma_Q^2)^{1/2}$. Next, define $y_j \equiv |e_{M_j} + e_{T_j} + e_{Q_j}|$. Consequently, the mean and variance of $|e_{M_j} + e_{T_j} + e_{Q_j}|$ are given by $E(y_j) = (2/\pi)^{1/2}\sigma$ and $\text{var}(y_j) = (1 - (2/\pi))\sigma^2$, where $E(\cdot)$ is the expectation operator and $\sigma \equiv (\sigma_M^2 + \sigma_T^2 + \sigma_Q^2)^{1/2}$. Because all the errors are assumed independent, and $\Delta S_i = 1/n \sum_{j=1}^n y_j$, the pdf of ΔS_i is given by

$$f(\Delta S) = \begin{cases} \frac{1}{\sqrt{2\pi}\sigma_{\Delta S}} e^{-\frac{(\Delta S - m_{\Delta S})^2}{2\sigma_{\Delta S}^2}}, & \Delta S \geq 0 \\ 0, & \Delta S < 0 \end{cases} \quad (1)$$

where $m_{\Delta S} \equiv ((2/\pi)(\sigma_M^2 + \sigma_T^2 + \sigma_Q^2))^{1/2}$ and $\sigma_{\Delta S} \equiv ((1 - (2/\pi))(\sigma_M^2 + \sigma_T^2 + \sigma_Q^2)/n)^{1/2}$.

Derivation of the Probability of Identification Error: The formulation of the pdf presented in (1) can be thought of as the pdf of the difference between the surveyed received power values corresponding to the location to that under examination. To evaluate the probability of error associated with identifying the location corresponding to k such that $\Delta S_k = \min_i[\Delta S_i]$, $1 \leq i \leq m$, the pdf corresponding to all surveyed locations needs to be specified.

Based on the problem formulation, the quantizing error is the only variable that affects the pdf characteristics for each of the m surveyed locations, where the statistical properties of e_{M_j} and e_{T_j} are assumed to be identical for all surveyed locations in a specific neighborhood.

Let σ_{Q_i} , $m_{\Delta S_i}$, $\sigma_{\Delta S_i}$, and correspondingly $f_i(\Delta S)$ denote the quantizing error standard deviation, the mean, standard deviation, and the pdf of ΔS_i , respectively, for $1 \leq i \leq m$. It is worth noting that as the distance between the location under examination and the surveyed location increases, σ_{Q_i} increases. Consequently, $m_{\Delta S_i}$ and $\sigma_{\Delta S_i}$ also increase. However, for $n > 1$, as σ_{Q_i} increases, $m_{\Delta S_i}$ increases at a faster rate than $\sigma_{\Delta S_i}$.

Let $\Pr(x)$ denote the probability of x , and let ΔS_c correspond to the location under examination closest to one of the m surveyed locations. Then, it can be shown that

$$\Pr\left(\Delta S_c < \min_{\substack{1 \leq j \leq m \\ j \neq c}} [\Delta S_j]\right) = \prod_{\substack{j=1 \\ j \neq c}}^m \left[\int_0^{\infty} f_c(x) \left(\int_x^{\infty} f_j(y) dy \right) dx \right].$$

Consequently, the probability of identification error is given by

$$P_e = 1 - \prod_{\substack{j=1 \\ j \neq c}}^m \left[\int_0^{\infty} f_c(x) \left(\int_x^{\infty} f_j(y) dy \right) dx \right]. \quad (2)$$

Remark 1: There is an apparent tradeoff between the distance between adjacent surveyed locations P_e and the accuracy of proposed power-matching algorithm. That is, as the distance between surveyed locations increases to a certain extent, accuracy in positioning decreases, however, m decreases, and consequently, P_e decreases. On the other hand, as the number

of SV under examination, n , increases, P_e decreases regardless the selected distance between selected surveyed locations.

C. Sensitivity Analysis in the Layout of the Surveyed Locations

The matrix $M(t)$ comprises information associated with discrete locations separated by a distance equal to δd (meters). Its obvious smaller values of δd would result in smaller quantizing errors or in a more precise positioning. However, when considering a two-dimensional (2-D) grid, the number of rows of the matrix $M(t)$ would increase at a rate inversely proportional to the square of δd . That is, if $\delta d/2$ is used instead of δd , then the number of rows would be four times larger than the one associated with δd . In the following, we examine the quantizing errors resulting from two points at a distance equal to δd . The analysis involved is based on the following hypothesis. This premise presumes that most of the SV signals are diffracted off an obstacle. The diffraction plane of a specific SV is defined to be the plane consisting of the SV, the surveyed location, and the corresponding point of diffraction. It is assumed that the minimum distance in the diffraction plane between a surveyed location and the obstacle is d_o (meters). This study also assumes Lee's approximate solution [37] to the knife-edge diffraction model. That is, the loss due to diffraction is given by

G_d (in decibels)

$$= \begin{cases} 0, & v \leq -1 \\ 20 \log(0.5 - 0.62v), & -1 < v \leq 0 \\ 20 \log[0.5 \exp(-0.95v)], & 0 < v \leq 1 \\ 20 \log[0.4 - \sqrt{0.1184 - (0.38 - 0.1v)^2}], & 1 < v \leq 2.4 \\ 20 \log\left(\frac{0.225}{v}\right), & v > 2.4 \end{cases}$$

where the Fresnel diffraction parameter $v = \alpha(2d_1d_2/\lambda(d_1 + d_2))^{1/2}$, where α is the radian angle between the straight line joining the SV and the point of diffraction and the straight line joining the point of diffraction and the GPS receiver in the diffraction plane, and λ is the wavelength in meters ($\lambda = 0.190425$ m for the L1 carrier frequency).

Let d_1 be the distance between a surveyed location and an obstacle in the diffraction plane, and d_2 is the distance between the SV and the obstacle. Because the SV is about 20 200 km away from the obstacle and its signal is diffracted, it can be assumed that $d_2 \gg d_1$. Thus, considering L1 carrier frequency, $v \cong 3.24\alpha\sqrt{d_1}$.

For power-matching application, the grid or the power map is thought of in a 2-D space laid on the navigation surface. Thus, two orthogonal projections of δds are involved, one in the direction of the obstacle-surveyed location in the diffraction plane, i.e., δd_{\parallel} , and the other perpendicular to the diffraction plane or to the direction of the obstacle-surveyed location, i.e., δd_{\perp} . As the deviation in δd_{\perp} does not affect the diffraction gain, δd_{\perp} is fixed. However, if the required quantizing accuracy is less than or equal to 1 m, then δd_{\perp} should be accordingly set to at least 1 m. In the following, the diffraction gain sensitivity is examined with respect to $\delta d_{\parallel} \equiv \delta d$. Let v^+ be the diffraction parameter corresponding to a horizontal distance $d_1 + \delta d$ away from obstacle. Then, $v^+ \cong v(1 + \delta d/d_1)^{1/2}$. Consequently, for a fixed value of δd , the diffraction parameter v or the diffraction

gain deviation G_d is largest whenever d_1 is smallest or $d_1 = d_o$. Simulation results show that if $1 \text{ m} \leq d_o < 2 \text{ m}$ and $\delta d = 0.2 \text{ m}$; $2 \text{ m} \leq d_o < 4 \text{ m}$ and $\delta d = 0.5 \text{ m}$; $4 \text{ m} \leq d_o (< 9 \text{ m})$ and $\delta d = 1 \text{ m}$, then the maximum diffraction gain deviation is approximately 1.26, or 1 dB. Thus, $\sigma_Q = 0.36$. As a consequence of the aforementioned analysis and to minimize the number of entries of the information matrix $M(t)$, the 2-D grid needs to be nonuniform.

Remark 2: Consider surveyed locations perpendicular to a specific diffraction plane associated with SV_1 . Then, the power received corresponding to SV_1 are approximately equal for the surveyed locations under consideration. However, based on the GPS SV constellation, the diffraction planes cannot be parallel at any specific location. Consequently, the power received from any other SV would vary among the surveyed locations under consideration, resulting in different power signatures.

D. Example

In [35], it is shown that when the UTSFM is used, the root mean square (rms) error in the modeled cumulative fade distribution, with respect to the fade distribution measured in Japan, is approximately 0.7 dB, or $\sigma_M \approx 1.18$. Furthermore, if $2 \text{ m} \leq d_o < 4 \text{ m}$ and $\delta d = 0.5 \text{ m}$, then $\sigma_Q = 0.36$. Thus, $P_{\text{avg}} \approx 1.52$, $m_{\Delta S} \approx 1$, and $\sigma_{\Delta S} \approx 0.75/\sqrt{n}$. Note that the thermal noise can be considered insignificant and thus neglected. Consequently, because $\sigma_M \approx 3.3\sigma_Q$, the region around the location under investigation, with a probability of error $< 2.3\%$, would be a sphere or disc of radius $\approx 2 \times 3.3 \times 0.5 = 3.3 \text{ m}$. Applying the power-matching algorithm, with power measurement from n different SVs, would significantly reduce the “size of the sphere” or disc, that is, $0.25 \text{ m} \leq$ absolute error $\ll 3.3 \text{ m}$. It is worth noting that the proposed algorithm can also be implemented in the CR to further reduce the position error estimated by the GPS receiver. As expected, the position accuracy is bounded by half the distance among the surveyed points.

E. Proposed Soft Aiding System Versus Sensor Aiding System

In this section, a comparative study between the proposed soft aiding system and sensor aiding system is presented. Four issues are considered, namely 1) hardware cost, 2) complexity of implementation, 3) performance, and 4) application domain.

- 1) *Hardware cost:* The sensor aiding system requires additional sensors with appropriate wiring, whereas the soft aiding system does not require any additional sensors. The employment of a gyro, in many sensor-aiding systems, costs relatively high and is not shockproof. This drawback makes such systems difficult to popularize in common vehicles.
- 2) *Complexity of implementation:* The sensor aiding systems usually require storage of 2-D road profile in a database for map matching or road profile recognition. The database of the road profile of most major cities and urban areas around the world are already available. Whereas,

the proposed soft aiding system requires topographical database of the terrains and buildings. This database is then used, along with the periodic profiles of the GPS satellites, to generate estimates for the received power for several points in the vicinity of the vehicle. Consequently, the realization of the database can be considered more complex than the one corresponding to the sensor aiding system. However, the database of both systems requires frequent updates.

- 3) *Performance:* The sensor aiding systems, which are based on integrating GPS and DR system, rely on measurements from gyros, compass or ABS, and wheel counters or odometer, or the inertial measurement unit. However, these measurements are unavoidably erroneous and result in inferior long-term accuracy until GPS signal is reestablished. The map-matching approach is generally used to reconcile inaccurate location data with digital map data. This approach depends heavily on the road curvatures. That is, within a straight road of a PD region, a DR can only project the location on the road. Thus, it can partially correct the lateral or horizontal dimension but not the vertical dimension. In addition, this approach typically suffers from feature detection failures, especially, when features are sparse or not recognizable [39], and can sometimes identify incorrect road segments [40]. Many experiments were conducted using sensor aiding systems with different signal processing algorithms. Recently, in [20], [39], and [41], the errors are reported to be in the range of 15 m for different experiments. In fact, the corresponding errors can be categorized as nonstationary. In particular, the errors can grow with distance traveled. Whereas the proposed soft aiding system does not depend on road curvature, and the corresponding errors can be categorized as stationary. It is also possible to identify incorrect position for specific locations. However, if the corresponding incorrect position is not within a small vicinity of the latest recorded location, then a corrective algorithm would disregard this incorrect update for its sudden large repositioning. Unlike the sensor aiding systems where identification relies on the existence of road curvature, the identification for proposed system can be executed almost continuously in the space domain, depending on the density of the surveyed locations in the power map (Fig. 2). Based on the theoretical example discussed in Section III-D, the absolute error corresponding to the proposed system should be less than 3.3 m.
- 4) *Application domain:* Most sensor aiding systems using map-matching algorithms and odometers (or wheel counters) encompass two inherent restrictions, namely 1) the system can only be installed on vehicles with wheels and 2) the navigation is restricted to specified tracks. Consequently, unless the track is prespecified, the map-matching algorithm fails when used on an all-track vehicle navigating haphazardly in a forest. In addition, such systems cannot be used by pedestrians. Whereas the proposed soft aiding system is not bounded to these two restrictions.

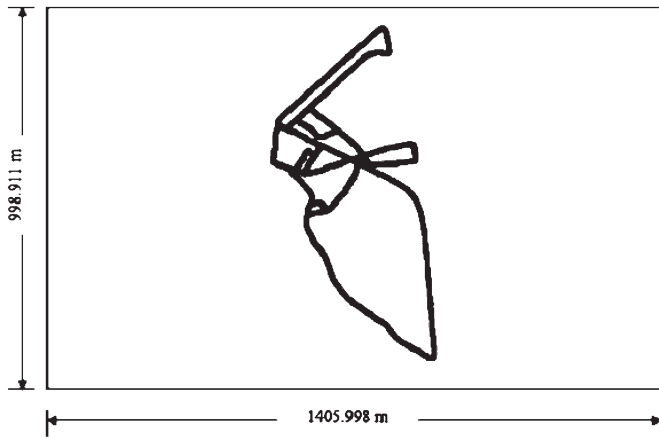


Fig. 4. Two-dimensional map of a neighborhood in Byblos City.

IV. EXPERIMENTAL WORK

A. Experimental Setup

In this subsection, we present the experiments conducted to examine the validity of the proposed methodology. It is worth noting that this experiment relies on the available measurements of the SNR values instead of power values. However, the noise level can be approximated to be constant for a specific time during the day and for a specific area. Consequently, for significant SNR values, the variations of the power values and SNR values are similar. The objective of the experiments is twofold: 1) They should show that there is some form of *consistent* SNR values if the GPS receiver would return to the same PD region after Δt , and 2) they should show *different* SNR values in different nearby PD regions. In other words, they should show that each road segment within the zoomed PD region has its *unique consistent* signature (SNR value). The experiments were conducted in the streets of a neighborhood of the city of Byblos, Lebanon (see Fig. 4). With the help of the Almanac data, a time slot in which there is a minimum number of GPS SVs above the city of Byblos was selected. The advantage of conducting the experiments at such a time was that the number of SVs would be critical, thus being unable to use one or more SVs would cause the GPS receiver to be roving in a PD or TD region. The best time slot was found to fall between 23:00:00 and 00:00:00. At this time slot, the number of GPS SVs above the city of Byblos ranged between four and five.

Finding the region in which the experiments were going to take place was the toughest part of all. It was desired to conduct the experiments in a region where there is an intersection of different road segments and where each road segment including the node of intersection falls in a PD region. This would make it almost impossible for the GPS receiver *alone* to predict which road segment it is roving in, even when map-matching algorithms are applied. After conducting extensive trial experiments in the chosen neighborhood of the city of Byblos at the chosen time slot, an “ideal” region was found. Fig. 5 zooms on the chosen region from the original map.

In this particular region, it was found that node N and its proximity constitute a PD region. It was necessary to rove far away from node N to enter a CR again. After selecting the time

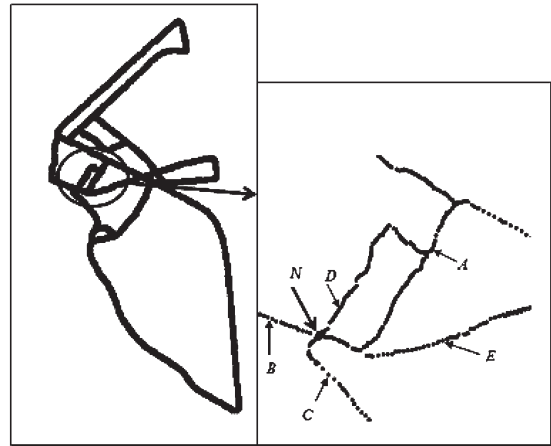


Fig. 5. Map of the region where the experiments were conducted.

at which the experiments will be conducted, and after deciding on the region at which the experiments will take place, two sets of experiments over two consecutive days were conducted. The experiments were aiming to show that each road segment within the zoomed PD region has its *unique consistent* signature (SNR values).

The experiments took place on February 20, 2001 and February 21, 2001. A Trimble Navigation PRO XRS receiver was mounted on a car to collect the points throughout the experiments. It is worth noting that the measured SNR corresponding to this specific experiment largely depends on the employed receiver type. The roving car started on February 20, 2001 at 21:24:02 at point A shown in Fig. 5 and moved in the following sequence: from point A to point B (in forward mode), from point B to point C (in reverse mode), from point C to point D (in forward mode), from point D to node N (in reverse mode), and finally, from node N to point E (in forward mode). On February 21, 2001, at 21:20:02, the “same” route was followed by starting at point A and ending at point E while preserving the order of the intermediate points B, C, and D. The points that were collected throughout the experiments were stored with the aid of a Trimble Navigation TSC1 Asset Surveyor, and the NMEA output messages were stored by connecting the PRO XRS Trimble Navigation GPS receiver to the COM1 port of a laptop PC and downloaded with the aid of a Hyper Terminal software.

After conducting the experiments over the two days, the data were transferred to the base station PC, and with the aid of the Lebanese American University Trimble Navigation Base Station, the data were differentially corrected through postprocessing. Then, using the Trimble Navigation Pathfinder Office Version 2.11 software, the points recorded in the two experiments were plotted separately while setting the map of that specific region of the city of Byblos as a background (see Figs. 6 and 7). It was noticed that the PD region and the CR were almost identical over the two days of the experiment. This means that the GPS receiver lost lock from the GPS SVs and gained it again at almost the same locations. This observation proves that there exists some form of “consistent” signatures of PD region and CR when the same locations are revisited after Δt . Afterward, a MATLAB code was written to

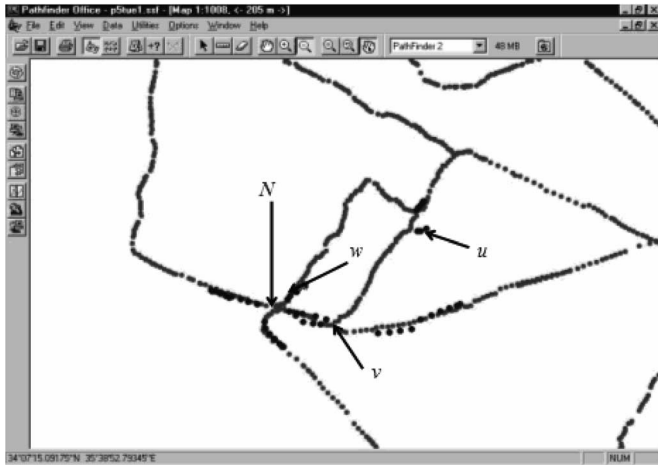


Fig. 6. Route of February 20, 2001.

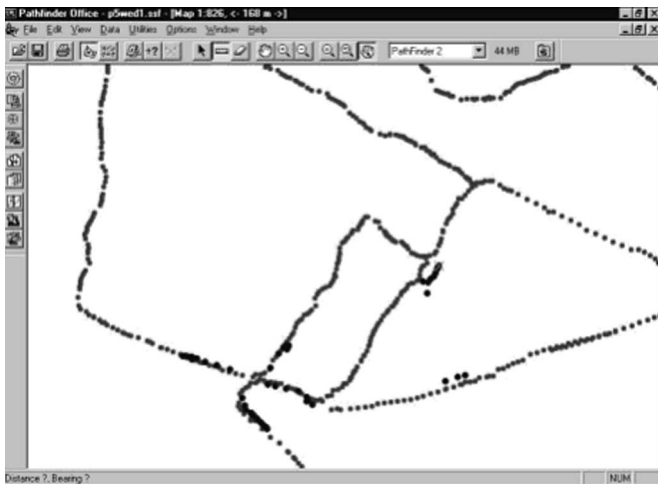


Fig. 7. Route of February 21, 2001.

extract the parameters of interest from the ASCII NMEA output messages. The data extracted were then tabulated and analyzed. Some samples of the data collected are presented in the next subsection.

B. Data Analysis and Observations

It was mentioned earlier that the aim of the experimental work conducted is to prove that there exists some form of unique and consistent signatures of nearby PD regions. Succeeding to do so will enable the GPS receiver to identify its position within PD regions based solely on the GPS data, thus eliminating the need to refer to external positioning systems. The parameters under consideration here will be the GPS SV positions as well as the SNR values of each GPS SV available. On one hand, the GPS SVs positions were taken care of by conducting the experiments at the same location with a time offset of Δt between the two consecutive days. By extracting the GPS SV positions (elevations and azimuths) from the GPGSV NMEA output message, it was noticed that all the SVs maintained their locations at $(t + \Delta t)$ throughout the two days. On the other hand, the SNR values of all the available GPS SVs were tabulated and analyzed separately.

TABLE I
SNR VALUES, ELEVATIONS, AND AZIMUTHS IN THE PD REGION BETWEEN POINTS U AND V IN DAY 1

Time Fix	#of SVs	PRN	SNR	PRN	SNR	PRN	SNR	PRN	SNR	PRN	SNR
212420	5	1	29 (4)	11	49 (24)	20	0 (0)	25	47 (22)	13	0 (0)
212421	5	1	30 (5)	11	46 (20)	20	0 (0)	25	46 (21)	13	0 (0)
212422	5	1	0 (0)	11	47 (22)	20	0 (0)	25	42 (17)	13	0 (0)
212423	5	1	0 (0)	11	47 (22)	20	0 (0)	25	45 (20)	13	0 (0)
212424	5	1	0 (0)	11	48 (23)	20	0 (0)	25	40 (15)	13	0 (0)
212425	5	1	47 (22)	11	47 (22)	20	0 (0)	25	41 (16)	13	0 (0)
212426	5	1	46 (21)	11	46 (21)	20	0 (0)	25	38 (13)	13	0 (0)
212427	5	1	47 (22)	11	47 (22)	20	0 (0)	25	43 (18)	13	0 (0)

Time Fix	#of SVs	PRN	Elev.	Azim.	PRN	Elev.	Azim.	PRN	Elev.	Azim.	PRN	Elev.	Azim.
212420	5	1	47	250	11	66	190	20	52	324	25	42	66
											13	18	242

TABLE II
SNR VALUES, ELEVATIONS, AND AZIMUTHS IN THE PD REGION BETWEEN POINTS U AND V IN DAY 2

Time Fix	#of SVs	PRN	SNR	PRN	SNR	PRN	SNR	PRN	SNR	PRN	SNR
212020	5	1	26 (1)	11	46 (20)	20	0 (0)	25	46 (21)	13	0 (0)
212021	5	1	0 (0)	11	48 (23)	20	0 (0)	25	42 (17)	13	0 (0)
212022	5	1	0 (0)	11	46 (21)	20	0 (0)	25	45 (20)	13	0 (0)
212023	5	1	0 (0)	11	48 (23)	20	0 (0)	25	39 (14)	13	0 (0)
212024	5	1	46 (21)	11	48 (23)	20	0 (0)	25	41 (16)	13	0 (0)
212025	5	1	48 (23)	11	46 (21)	20	0 (0)	25	41 (16)	13	0 (0)
212026	5	1	43 (18)	11	46 (21)	20	0 (0)	25	45 (20)	13	0 (0)
212027	5	1	38 (13)	11	48 (23)	20	0 (0)	25	40 (15)	13	0 (0)

Time Fix	#of SVs	PRN	Elev.	Azim.	PRN	Elev.	Azim.	PRN	Elev.	Azim.	PRN	Elev.	Azim.
212020	5	1	47	250	11	66	190	20	53	324	25	42	66
											13	18	242

TABLE III
SNR VALUES, ELEVATIONS, AND AZIMUTHS IN THE PD REGION BETWEEN POINTS U AND V IN DAY 2

Time Fix	#of SVs	PRN	SNR	PRN	SNR	PRN	SNR	PRN	SNR	PRN	SNR
212015	5	1	0 (0)	11	45 (20)	20	30 (5)	25	45 (20)	13	0 (0)
212016	5	1	0 (0)	11	44 (19)	20	28 (3)	25	45 (20)	13	0 (0)
212017	5	1	0 (0)	11	44 (19)	20	0 (0)	25	45 (20)	13	0 (0)
212018	5	1	0 (0)	11	47 (22)	20	0 (0)	25	45 (20)	13	0 (0)
212019	5	1	0 (0)	11	49 (24)	20	0 (0)	25	45 (20)	13	0 (0)

Time Fix	Total SVs	PRN	Elev.	Azim.	PRN	Elev.	Azim.	PRN	Elev.	Azim.	PRN	Elev.	Azim.
212015	5	1	47	250	11	67	190	20	53	324	25	42	66
											13	18	242

We will start with showing that there exists some form of a consistent signature for the same PD region when visited at two different time instants with a time offset of Δt . Tables I and II show the SNR values, the elevations, and the azimuths of all available GPS SVs in the PD region between points u and v (see Fig. 6). The elevations and azimuths of all the GPS SVs are reported for 1 s only, and they are the same throughout the subsequent seconds. It is worth noting that the maximum SNR reported by the employed GPS receiver is 50 dB, and all SNR values falling below 25 dB are reported as 0 dB. Thus, when normalizing to a range of [0 dB, 25 dB], that is subtracting 25 dB from all SNR > 25 dB, hence, a [25 + x] dB would result in x dB. The values between parentheses of the SNRs in Tables I-IV correspond to the normalized values.

The following conclusions could be drawn from these tables. First, the time fix indicates that on February 20, 2001 at 21:24:21, the GPS receiver was roving inside the PD region

TABLE IV
SNR VALUES, ELEVATIONS, AND AZIMUTHS IN THE PD REGION
BETWEEN POINTS W AND N IN DAY 2

Time Fix	# of SVs	PRN	SNR	PRN	SHR	PRN	SNR	PRN	SHR	PRN	SNR
212120	5	1	42 (17)	11	43	20	49 (24)	25	0 (0)	13	0 (0)
212121	5	1	40 (15)	11	45 (20)	20	50 (25)	25	0 (0)	13	0 (0)
212122	5	1	29 (4)	11	47	20	45 (20)	25	0 (0)	13	0 (0)
212123	5	1	35 (10)	11	51	20	42 (17)	25	0 (0)	13	0 (0)
212124	5	1	38 (13)	11	52	20	39 (14)	25	0 (0)	13	0 (0)

Time Fix	Total SVs	PRN	Elev.	Azim.	PRN	Elev.	Azim.	PRN	Elev.	Azim.	PRN	Elev.	Azim.
212120	5	1	47	250	11	66	189	20	53	324	25	42	66
											13	19	242

between points u and v, whereas it was roving within the same PD region on February 21, 2001 at 21:20:21 (i.e., time offset Δt). Second, the GPS SVs maintained their previous locations (elevations and azimuths) after a time offset of Δt . Third, almost all of the SNR values match between the two days of the experiments. There are only two “major” mismatches, which are highlighted in black cells associated with $SV_{PRN=1}$. Other less significant mismatches are associated with $SV_{PRN=25}$. Now, to explain these variations and, in particular, these two major mismatches, it should be recalled that the experiments were conducted while mounting the GPS receiver on a roving car. Thus, even though the experiments were synchronized in time over the two days to have time offset of Δt , it was extremely difficult to synchronize the experiments in space and time over the two days, i.e., to be “exactly” at the same position over the two days at $(t + \Delta t)$. This explanation is strengthened by noting that the SNR values recorded at the seconds adjacent to this mismatch are identical. Thus, it seems that the car was displaced in position by a few meters and seconds over the two days. In Tables I and II, it can be noticed that out of the 40 recorded SNRs, 38 recordings are “closely” matched. After comparing all the SNR values between the two tables, we can conclude that there exists some form of consistent SNR values within the same PD region. In other words, the PD region under consideration has its consistent signature.

To check for the uniqueness of the signature of two different PD regions, another set of experiments should be conducted and analyzed. The experiments should simply compare the SNR values between two different PD regions while maintaining the GPS SV positions at the same locations. Tables III and IV show the SNR values, the elevations, and the azimuths of all available GPS SVs in two different PD regions within the same day (February 21, 2001). Table III shows the data recorded in the PD region between points u and v, whereas Table IV shows the data recorded in the PD region between point w and node N. Again, the elevations and azimuths are reported for 1 s only, as they are the same for the subsequent seconds in the tables.

By analyzing Tables III and IV, we could conclude that there exist a significant number of “major” mismatches (identified by black cells) among the SNR values between the two PD regions. Three of the SV SNRs completely disagree between the two locations. In conclusion, out of 25 recorded SNRs, there are 15 major mismatches. Tables V and VI present the standard deviations of the SNR values among all available SVs. It can be noted that, except for the value corresponding to the mismatch

TABLE V
STANDARD DEVIATION (STD) OF THE SNR VALUES
IN THE i TH ROW OF TABLES I AND II

Row#	1	2	3	4	5	6	7	8
STD	1.82	3.27	1.52	2.83	9.29	0.71	3.7	4.09

TABLE VI
STANDARD DEVIATION (STD) OF THE SNR VALUES
IN THE i TH ROW OF TABLES III AND IV

Row#	1	2	3	4	5
STD	15.93	16.16	14.28	13.97	13.73

in row 5 in Tables I and II, the SNR deviations of Tables I and II are *significantly* smaller than the SNR deviations of Tables III and IV. Thus, it can be concluded that each PD region has its unique signature. Many other similar experiments were conducted, which are not reported in this paper, and resulted in similar conclusions. A more reliable identification measure is presented in the next section.

C. Implementation of the Proposed Algorithm

Experimental Setup: In this section, the proposed algorithm is applied partially to the data given in Tables I–IV. Because only SNR values are available and the error and noise statistics can be assumed to be stationary over the small time period considered in Tables I–IV, analysis of SNR values is considered instead of the power values. The maximum SNR of the employed GPS receiver is equal to 50 dB, and SNR values less than or equal to 25 dB result in 0 dB. As a first step, the SNRs need to be normalized. As presented in the previous subsection, 25 dB must be subtracted from all the SNRs greater than or equal to 25 dB. Consequently, the normalized maximum SNR $A = 25$ dB.

As presented in the previous subsection, Tables I, II, and IV are the results of experiments executed within the same vicinity and at slightly different time periods. Tables I and II include data corresponding to two close trajectories executed in two “analogous” time periods. Table IV includes data of a different trajectory and at a slightly different time period. Note that because Table III includes data corresponding to a close trajectory, as in Tables I and II, but at different time periods, its corresponding data would not be considered. In this experimental simulation, the data of Table I are considered to reflect the measured SNRs and the data of Tables II and IV correspond to the information matrix $M(t)$, which is assumed to be estimated at the same time period of Table I. It is also assumed that the data of Table II are the nominal SNRs corresponding to the measured SNRs of Table I. Let $S_{m,i,j}$ denote the SNR of Table m , row i of SV PRN j , for $m = 2$ or 4, $1 \leq i \leq 8$, and $j = 1, 11, 20, 25$, or 13. Similarly, let $\hat{S}_{1,i,j}$ denote the SNR of Table I. The time argument is dropped for compactness. Table VII shows the corresponding percentage of the mean of absolute errors (MAE) $\%P_e(i)$ associated with $S_{m,i,j}$ and $\hat{S}_{1,i,j}$. It is worth noting that the distance traveled between u and v (Tables I and II) is less than 50 m within 8 s. Thus, the average value between two consecutive rows,

TABLE VII
PERCENTAGE OF MAE $\%P_e(i)$

	$\hat{S}_{2,1,j}$	$\hat{S}_{2,2,j}$	$\hat{S}_{2,3,j}$	$\hat{S}_{2,4,j}$	$\hat{S}_{2,5,j}$	$\hat{S}_{2,6,j}$	$\hat{S}_{2,7,j}$	$\hat{S}_{2,8,j}$	$\hat{S}_{4,1,j}$	$\hat{S}_{4,2,j}$	$\hat{S}_{4,3,j}$	$\hat{S}_{4,4,j}$	$\hat{S}_{4,5,j}$
$\hat{S}_{1,1,j}$	6.4	8.0	7.2	10.4	19.2	22.4	15.2	13.6	52.0	49.6	35.2	37.6	38.4
$\hat{S}_{1,2,j}$	3.2	9.6	5.6	12.0	19.2	19.2	12.0	13.6	47.2	44.8	35.2	39.2	40.0
$\hat{S}_{1,3,j}$	5.6	0.8	3.2	3.2	18.4	20.0	17.6	12.8	49.6	47.2	32.8	38.4	39.2
$\hat{S}_{1,4,j}$	3.2	3.2	0.8	5.6	20.8	22.4	15.2	15.2	52.0	49.6	35.2	40.8	41.6
$\hat{S}_{1,5,j}$	8.0	1.6	5.6	0.8	17.6	20.8	20.0	10.4	48.8	46.4	32.0	36.0	36.8
$\hat{S}_{1,6,j}$	22.4	19.2	21.6	20.0	1.6	1.6	7.2	8.8	39.2	40.0	43.2	39.2	35.2
$\hat{S}_{1,7,j}$	23.2	21.6	22.4	19.2	4.0	4.0	8.0	9.6	35.2	36.0	40.8	36.8	32.8
$\hat{S}_{1,8,j}$	20.8	19.2	20.0	21.6	3.2	3.2	5.6	10.4	40.8	41.6	44.8	40.8	36.8

in Tables I and II, is about 6 m. Thus, $\%P_e(i)$ is approximated as follows:

$$\%P_e(i) \cong \frac{\frac{1}{5} \sum_{j=1,11,20,25,13} |S_{m,i,j} - \hat{S}_{1,i,j}|}{25} \times 100\%.$$

Performance Analysis: By examining Table VII, it can be noticed that the minimum value of $\%P_e(i)$ is greater than 30% when comparing the different locations corresponding to Tables I and IV. As expected, these large values indicate the dissimilarity among the different locations associated with Tables I and IV. Whereas, the relatively small values of $\%P_e(i)$ (shown in bold, where $\%P_e(i) < 5\%$), which are the minimum values in each row, indicate resemblance associated with Tables I and II of the same track. Unfortunately, the two trajectories associated with Tables I and II could never be executed with perfect time synchronization, and because these experiments were conducted in PD region, the exact positions at each time instant could not be available. However, due to the high correlations, or equivalently, the relatively small values of $\%P_e(i)$, one can conclude that the time trajectory associated with Table I must be delayed by about 1 s (except for the starting point) when comparing it to the trajectory associated to Table II. The results presented in Table VII illustrate the potential of the proposed power matching methodology.

V. CONCLUSION

In this paper, it is shown that a power-matching methodology, without the integration of any other external sensor, can be used for GPS coverage extension. Four different experiments supporting consistency and distinctiveness of signatures were presented. In particular, it was shown that when the GPS receiver returned to a certain PD region after Δt , which is twice the orbital period of the constellation of GPS SVs, the GPS receiver experienced the same conditions of darkness. That is, when the same track was followed throughout two consecutive days having a time offset of Δt , the SNR values reported for all the available GPS SVs were almost identical. Nevertheless, these values were unique in different road segments emanating from the same node (within the same proximity) due to the different geometrical distribution of the surrounding terrains

and buildings. This has led us to conclude that each PD region within the same proximity has its unique consistent signature. If such a signature could be revealed while the GPS receiver roves into a certain PD region, then it could be relied on the GPS data and power-matching algorithms to *solely* identify one's location. The latter was supported by basic statistical analysis and by applying the proposed power-matching algorithm to realistic experimental data, where it is shown that GPS coverage can be extended. The advantages of applying this method for position determination over sensor aiding systems are threefold: 1) Using the GPS data alone along with power-matching techniques would eliminate the need to couple the GPS receiver with external sensors. Thus, the GPS receiver, a suitable topographic database, and appropriate power-matching algorithms would be sufficient and reliable enough for position determination. 2) Unlike the sensor aiding systems, the identification does not rely on road curvatures but can be rather implemented continuously. 3) This new proposed system, which is not restricted to prespecified tracks and distance-measurement sensor, could be useful for a wider application domain. Employing the proposed method requires topographical database of the terrains and buildings for the urban areas of interest. Such a database could be constructed and frequently updated with the aid of aerial images and ArcView 3-D Analyst [38].

ACKNOWLEDGMENT

The authors would like to thank the reviewers and the Associate Editor for their patience and constructive suggestions in improving the presentation of this manuscript.

REFERENCES

- [1] C. Drane and C. Rizos, *Positioning Systems in Intelligent Transportation Systems*. Norwood, MA: Artech House, 1998.
- [2] Y. Zhao, "Mobile phone location determination and its impact on intelligent transportation systems," *IEEE Trans. Intell. Transp. Syst.*, vol. 1, no. 1, pp. 55–64, Mar. 2000.
- [3] F. Gustafsson, F. Gunnarsson, N. Bergman, U. Forssell, J. Jansson, R. Karlsson, and P.-J. Nordlund, "Particle filters for positioning, navigation, and tracking," *IEEE Trans. Signal Process.*, vol. 50, no. 2, pp. 425–437, Feb. 2002.
- [4] C. R. Drane, *Positioning Systems: A Unified Approach*, 1st ed. New York: Springer-Verlag, 1992.
- [5] S. Saab, "A map-matching approach for train positioning—Part I: Development and analysis," *IEEE Trans. Veh. Technol.*, vol. 49, no. 2, pp. 467–475, Mar. 2000.
- [6] —, "A map-matching approach for train positioning—Part II: Application and experimentation," *IEEE Trans. Veh. Technol.*, vol. 49, no. 2, pp. 476–484, Mar. 2000.
- [7] A. Waxman, J. LeMoigne, and B. Scinvasan, "A visual navigation system for autonomous land vehicles," *IEEE J. Robot. Autom.*, vol. RA-3, no. 2, pp. 124–141, Apr. 1987.
- [8] Y. Yagi, Y. Nishizawa, and M. Yachida, "Map-based navigation for a mobile robot with omnidirectional image sensor COPIS," *IEEE Trans. Robot. Autom.*, vol. 11, no. 5, pp. 634–648, Oct. 1995.
- [9] R. French and M. Lang, "Automatic route control system," *IEEE Trans. Veh. Technol.*, vol. VT-22, no. 2, pp. 36–41, May 1973.
- [10] T. Lezniak, R. Lewis, and R. McMillen, "A dead-reckoning/map-correlation system for automatic vehicle tracking," *IEEE Trans. Veh. Technol.*, vol. VT-26, no. 1, pp. 47–60, Feb. 1977.
- [11] D. King, "LANDFALL: A high-resolution automatic vehicle location system," *GE J. Sci. Technol.*, vol. 45, no. 1, pp. 34–44, 1978.
- [12] E. G. Blackwell, "Overview of differential GPS methods," in *Global Positioning Systems*, vol. 3. Washington, DC: The Institute of Navigation, 1986, pp. 89–100.

- [13] E. J. Krakiwsky, C. B. Harris, and R. V. C. Wong, "A Kalman filter for integrating dead reckoning, map-matching, and GPS positioning," in *Proc. IEEE Position Location Navigat. Symp.*, 1988, pp. 39–46.
- [14] J. Tanka, "Navigation system with map-matching method," in *Proc. SAE Int. Congr. Expo.*, 1990, pp. 45–50.
- [15] R. French, "Intelligent vehicle/highway systems in action," *ITE J.*, vol. 60, no. 2, pp. 23–31, Nov. 1990.
- [16] H. Degawa, "A new navigation system with multiple information sources," in *Proc. Vehicle Navigat. Inf. Syst. Conf.*, 1992, pp. 143–149.
- [17] P. G. Mattos, "Integrated GPS and dead reckoning for low-cost vehicle navigation and tracking," in *Proc. Vehicle Navigat. Inf. Syst. Conf.*, 1994, pp. 569–574.
- [18] J. S. Kim, "Node based map-matching algorithm for car navigation system," in *Proc. Int. Symp. Automot. Technol. Autom.*, 1996, pp. 121–126.
- [19] T. Jo, M. Haseyama, and H. Kitajima, "A map-matching method with the innovation of the Kalman filtering," *IEICE Trans. Fundam. Electron. Commun. Comput. Sci.*, vol. E79-A, no. 11, pp. 1853–1855, Nov. 1996.
- [20] S. Kim and J.-H. Kim, "Adaptive fuzzy-network-based C-measure map-matching algorithm for car navigation system," *IEEE Trans. Ind. Electron.*, vol. 48, no. 2, pp. 432–441, Apr. 2001.
- [21] J.-S. Pyo, D.-H. Shin, and T.-K. Sung, "Development of a map matching method using the multiple hypothesis technique," in *Proc. IEEE Intell. Transp. Syst.*, Aug. 2001, pp. 23–27.
- [22] R. Joshi, "Novel metrics for map-matching in in-vehicle navigation systems," in *Proc. IEEE Intell. Vehicle Symp.*, Jun. 2002, pp. 36–43.
- [23] L. Jie and F. Meng-yin, "Research on route planning and map-matching in vehicle GPS/dead-reckoning/electronic map integrated navigation system," in *Proc. IEEE Intell. Transp. Syst.*, Oct. 2003, pp. 1639–1643.
- [24] D. M. Lin and J. B. Y. Tsui, "A software GPS receiver for weak signals," in *Proc. IEEE MTT-S Microw. Symp. Dig.*, 2001, pp. 219–2142.
- [25] M. L. Psiaki, "Block acquisition of weak GPS signals in a software receiver," in *Proc. ION-GPS*, Salt Lake City, UT, Sep. 2001, pp. 2838–2850.
- [26] P. H. Madhani, P. Axelrad, K. Krumvieda, and J. Thomas, "Application of successive interference cancellation to the GPS pseudolite near-far problem," *IEEE Trans. Aerosp. Electron. Syst.*, vol. 39, no. 2, pp. 481–488, Apr. 2003.
- [27] N. I. Zeidan and J. L. Garrison, "Unaided acquisition of weak GPS signals using circular correlation or double-block zero padding," in *Proc. IEEE Position Location Navigat. Symp.*, 2004, pp. 461–470.
- [28] S. S. Saab and Z. M. Kassas, "Map-based land vehicle navigation system with DGPS," in *Proc. IEEE Intell. Vehicle Symp.*, Jun. 2002, pp. 209–214.
- [29] E. D. Kaplan, *Understanding GPS Principles and Applications*. Boston, MA: Artech House, 1996.
- [30] *PRO XR/XRS Receiver Manual*, Trimble Navigation Limited, Sunnyvale, CA, 1998.
- [31] *Community Base Station System*. Sunnyvale, CA: Trimble Navigation, 1997.
- [32] A. Leick, *GPS Satellite Surveying*. New York: Wiley, 1995.
- [33] *Pathfinder Office Version 2.11*. Sunnyvale, CA: Trimble Navigation, 1998.
- [34] *TSCI Asset Surveyor*. Hampshire, U.K.: Trimble Navigation Europe Limited, 1998.
- [35] R. Akturan and W. J. Vogel, "Path diversity for LEO satellite-PCS in the urban environment," *IEEE Trans. Antennas Propag.*, vol. 45, no. 7, pp. 1107–1116, Jul. 1997.
- [36] R. Klukas, G. Lachapelle, C. Ma, and G.-I. Jee, "GPS signal fading model for urban centers," *Proc. Inst. Elect. Eng.—Microw. Antennas Propag.*, vol. 150, no. 4, pp. 245–252, Aug. 2003.
- [37] W. C. Y. Lee, *Mobile Communications Engineering*. New York: McGraw-Hill, 1985.
- [38] J. S. Greenfeld, "Matching GPS observations to locations on a digital map," in *Proc. 81st Annu. Meeting Transp. Res. Board, Nat. Res. Council*, Washington, DC, 2002. CD-ROM.
- [39] K. W. Lee, W. S. Wijesoma, and J. Ibanez-Guzman, "Map aided SLAM in neighbourhood environments," in *Proc. IEEE Intell. Vehicles Symp.*, Jun. 14–17, 2004, pp. 836–841.
- [40] M. A. Quddus, W. Y. Ochieng, L. Zhao, and R. B. Noland, "A general map matching algorithm for transport telematics applications," *GPS Solut.*, vol. 7, no. 3, pp. 157–167, 2003.
- [41] Q. Shengbo, D. Keliang, and L. Qingli, "An effective GPS/DR device and algorithm used in vehicle positioning system," in *Proc. IEEE Intell. Transp. Syst.*, 2003, vol. 1, pp. 632–636.
- [42] W. Holzapfel, M. Sofsky, and U. Neuschaefer-Rube, "Road profile recognition for autonomous car navigation and Navstar GPS support," *IEEE Trans. Aerosp. Electron. Syst.*, vol. 39, no. 1, pp. 2–12, Jan. 2003.



Samer S. Saab (S'92–M'93–SM'98) received the B.S., M.S., and Ph.D. degrees in electrical engineering and the M.A. degree in applied mathematics from the University of Pittsburgh, Pittsburgh, PA, in 1988, 1989, 1992, and 1990, respectively.

He joined the Faculty of the Lebanese American University, Byblos, Lebanon, in 1996. He has been an Associate Professor since 2001, and he is currently the Chairperson of the Department of Electrical and Computer Engineering, Lebanese American University. From 1993 to 1995, he was a Consulting Engineer at Union Switch and Signal, Pittsburgh, and from 1995 to 1996, he was a System Engineer at ABB Daimler-Benz Transportation, Inc., Pittsburgh, where he was involved in the design of automatic train control and positioning systems. His research interests include iterative learning control, Kalman filtering, navigational positioning systems, and wireless communications.

Dr. Saab is on the Editorial Board of the IEEE TRANSACTIONS ON CONTROL SYSTEMS TECHNOLOGY. He is also serving on the IEEE Control Systems Society Conference Editorial Board.



Zaher M. Kassas (S'98) received the B.E. degree in electrical engineering from the Lebanese American University, Byblos, Lebanon, in 2001 and the M.S. degree in electrical engineering from the Ohio State University, Columbus, OH, in 2003.

He is currently a Research and Development Engineer with the Control Design and Simulation Group at National Instruments, Austin, TX. From 2002 to 2004, he was a Graduate Research Associate with the Collaborative Center of Control Science, Ohio State University, where he was involved with the design

of nonlinear Bayesian estimation filters for uninhibited autonomous vehicles for in-surveillance and out-of-surveillance mobile ground target tracking. His research interests include detection and estimation, filtering, and stochastic control.